energies

MDPI

Review

A Review of Fully Integrated and Embedded Power Converters for IoT

Anna Richelli [1,*,†], Mohamed Salem [2,†] and Luigi Colalongo [1,†]

[1] Department of Information Engineering, University of Brescia, via Branze 38, 25123 Brescia, Italy; luigi.colalongo@unibs.it
[2] School of Electrical and Electronic Engineering, Universiti Sains Malaysia, Nibong Tebal 14300, Penang, Malaysia; salemm@usm.my
* Correspondence: anna.richelli@unibs.it; Tel.: +39-030-371-5501
† The authors contributed equally to this work.

Abstract: The Internet of Things (IoT) has found application in many components of implantable medical devices, wearable smart devices, monitoring systems, etc. The IoT devices are conventionally battery powered, even though, in several low power applications, they can also be powered using energy harvesting technology. Independently of the power sources (if batteries or environment), efficient and robust power converters must be designed to provide the small and distributed energy required by such IoT devices. This review paper will first provide an overview about the power consumption in IoT devices; second, it will discuss the most recent research and advance in the field of fully-integrated or embedded DC/DC converters, starting from high-performance integrated charge pumps or embedded inductive boost converters for specific harvesting sources (temperature, solar, and so on), to novel DC/DC converters for multiple energy sources.

Keywords: Internet of Things; sensor networks; power supply; energy harvesting; battery life; power converters; integrated circuits

Citation: Richelli, A.; Salem, M.; Colalongo, L. A Review of Fully Integrated and Embedded Power Converters for IoT. *Energies* **2021**, *14*, 5419. https://doi.org/10.3390/en14175419

Academic Editor: Woojin Choi

Received: 14 July 2021
Accepted: 18 August 2021
Published: 31 August 2021

1. Introduction

The development of technologies within the Internet of Things (IoT) framework is realizing the connected world. All the component units of IoT devices are connected for information and data exchange, thereby forming a larger global network. These "things" could be components of a complex system used for different purposes, such as smart agriculture, healthcare, vehicles, satellites, science experiments, etc. In Figure 1, a portrait of the ubiquitous connected electronics is painted to give a visual idea. This pervasive and widespread potential usage leads the semiconductor industry to perceive IoT as a very promising growth area. On the other, IoT applications demand stringent requirements on the form factor of the resulting electronics and their power consumption. The need of sensor ubiquity is probably the main issue in IoT. Indeed, in several applications, although the power supply can be delivered by batteries, frequent recharges of batteries are not desirable. Moreover, in the case of energy harvesting from the environment, efficient conversion and management of this energy is mandatory. Furthermore, note that another important characteristic to allow for sensor ubiquity, is the flexibility, versatility and adaptability of the DC/DC converters: for example, the capability to convert the power from multiple energy sources is especially appealing in IoT applications.

To get a practical overview of the energy issues in an IoT system, we can consider Figure 2. The possible energy sources can be, between the other ones, solar, thermal, vibration, or wind; a common consideration is that the energy extracted from the environment is a kind of raw energy which must be converted and stored, in order to be useful in an electrical system. For example, a thermopile exposed to a few degrees of temperature difference can provide a good level of current but only a few hundreds of mV of voltage [1,2]. Therefore, the second block of the overall system, as depicted in the figure, is

energy storage, which can be represented by batteries, flexible and paper batteries, capacitors and supercapacitors [3,4]. Finally, it is worth investigating which are the most energy-starved subsystems. For example, sensors and analog or digital signal conditioning can be designed to be low power, but it is important to know the energy required by the transceiver, the communication protocols (bluetooth, zigbee, bluetooth low energy, etc.) and the required data rate [5]. These are, of course, application-dependent parameters, and it is important to have a precise overview of them, before and during the design phase.

Figure 1. IoT is connecting the world.

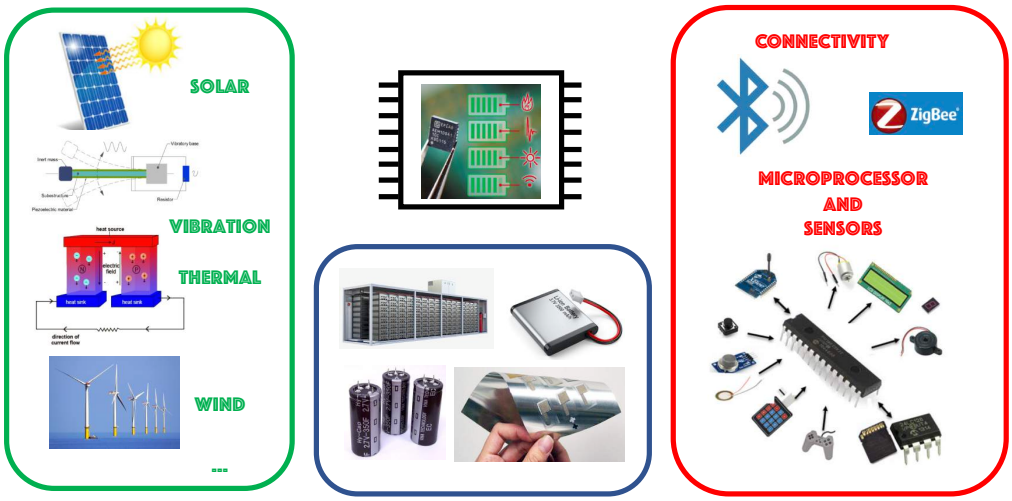

Figure 2. The energy in IoT systems.

This paper aims to

- get an overview of the energy issues in an IoT system;
- introduce the most recent and relevant embedded topologies which can be used for power conversion and management;
- get an overview on the power conversion issues; and
- present possible solutions for IoT nodes powered by the energy harvesting technique, with a particular focus on the converters exploiting multiple power sources.

This paper has been organized as follows. Section 2 provides an overview about the power consumption in IoT devices. Section 3 presents the main topologies used for the en-

ergy harvesting, in particular in the case of the Internet of Things. In Section 4, several converters for specific harvesting sources (temperature, solar, and so on) are depicted. Section 5 presents DC/DC converters for multiple energy sources. Finally, Section 6 concludes the paper.

2. Power Consumption in IoT Devices

IoT sensors are "set and forget" devices intended for prolonged performance on small batteries at low voltages and currents. Therefore, knowing the power consumption of an IoT device is mandatory for the proper choice of the batteries or of the energy storage elements, but the characterization of the consumption is complicated because all the elements (sensors, actuators, microprocessors, and transceiver) must be considered along with their operating conditions. A typical IoT device contains one or more sensors and actuators, a microprocessor, and a radio chip that can send and receive signals at some standard operating voltage, such as +3.0 to +3.5 V dc. However, it can also wait in a standby mode for an activating signal from a user checking on the IoT device with, for instance, a cellphone. Furthermore, that device may be functioning at +0.5 V dc or less in a kind of sleep mode to save power, especially for long-duration, remote monitoring applications where the battery's power must be maintained. Some remote monitoring applications, for example, may require that an IoT device remain powered by its battery for 20 years or more, and achieving extremely low power consumption is critical for these devices. The power required to operate a wireless node can be grouped into power need for data acquisition, power need for processing data, and power need for data communication. Some sensors can acquire data, which are processed by a controller unit and then transmitted though a wireless channel. Being that this process is continuously repeated, it is believed that the duty cycle is fundamental in determining the energy consumption because the shorter the duty cycle (achievable through reducing the active time or prolonging the idle periods), the lower the average energy usage. In any case, among all the IoT components, one of the most consuming is the transceiver, and its power consumption is also dependent on the communication technology: Wi-Fi, Long Range (LoRA), Narrow Band IoT (NB-IoT), LTE-M (Long Term Evolution-Machine), Sigfox, Weightless, Bluetooth, ZigBee, Bluetooth Low Energy (BLE), and so on. Many works indeed focus on the power optimization of the communication side. For example, in [6] the power consumed by an IoT sensor node is evaluated from a different point of view and the consumption is divided into four terms:

$$P_{DEV} = P_{NET} + P_{ACQ} + P_{PRC} + P_{SYS} \quad (1)$$

for data communication, or networking P_{NET}; for data sensing or acquisition P_{ACQ}; for data handling or processing, P_{PRC}; and for system management task P_{SYS}. P_{NET} is influenced by the energy to send a radio message and by the time between consecutive message. P_{ACQ} can be split into two terms: the first one is related to the regular acquisition of data from the sensor, and the second one comes from the event triggered acquisition. P_{PRC} depends on the algorithm complexity, while P_{SYS} is intended for the management of the tasks in the system, such as implementation of a real-time OS or waking the system at periodic wake-ups. In [7], instead, a detailed comparison between the different communication technologies for IoT devices is discussed: the comparison is in terms of range, data rate, battery life, security, and installation cost. For the sake of clarity, the main parameters of the comparison are listed in Table 1.

Finally, in [8], the impact of the IoT wireless node communicating with the cloud is evaluated, showing that the cloud energy consumption is much less than the IoT part, as schematically drawn in Figure 3.

Table 1. Communication technologies for IoT devices.

Technology	Range	Data Rate	Battery Life	Security	Installation Cost
LoRA	≤50 km	0.3–38.4 kbps	8–10 years	High	Low
NB-IoT	≤50 km	≤100 kbps	1–2 years	High	Low
LTE-M	≤200 km	0.2–1 Mbps	7–8 years	High	Moderate
Sigfox	≤50 km	100 bps	7–8 years	High	Moderate
Weightless	<5 km	100 kbps	Very Long	High	Low
Bluetooth	≤50 m	1 Mbps	Few Months	High	Low
Zigbee	≤100 m	250 kbps	5–10 years	Low	Low
Satellite	>1500 km	100 kbps	Very Low	High	Costly

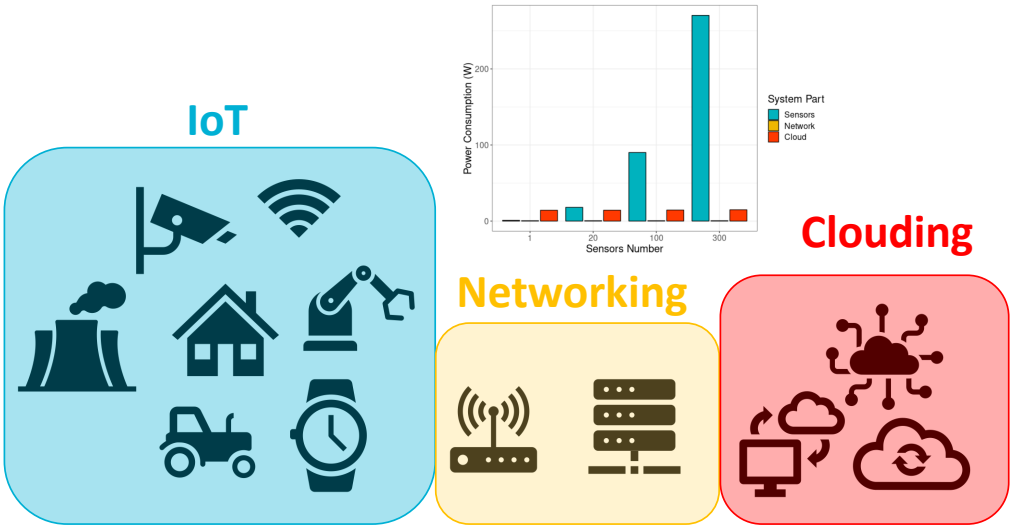

Figure 3. Power consumption of IoT nodes.

As a final consideration, many IoT devices are virtually systems in themselves, capable of measuring current and power at low voltages with high accuracy.

3. Circuital Architectures of the Main Converters' Topologies Used in IoT

Modern sensor networks, processors, I/O circuits, and memories are mainly based on low-voltage/ultra-low-voltage circuit techniques. However, the need for higher internal voltages in most systems on chip, that are based on these low voltage techniques, demand the need for an efficient DC/DC conversion system. To generate larger voltages than the supply voltage that is available, boost DC/DC converter circuits are normally used, especially during non-volatile memories programming, or in low-voltage switched-capacitor systems, and so on. The conversion can be made by basically two classical topologies, as shown in Figure 4: charge pumps and step-up inductive converters.

DC/DC conversion in ICs is mainly achieved using charge pumps, most often based on the Dickson architecture [9]. The maximum output voltage of these charge pumps is approximately (N+1).(Vdd-VT), where N represents the number of stages, Vdd represents the supply voltage, and VT represents the threshold voltage of the diode-connected MOS transistors. The main limitations of these converters is their inefficiency in transferring charge; therefore, several studies try to improve the voltage gain in every stage and to investigate the energy consumption [10–15]. Regarding the classical Dickson charge pump (shown in Figure 4), the main novelty of the recent architectures lies in the use of pass transistors (switches) instead of diode-connected MOS, and/or in more complex timing schemes, as in [10,15,16], or in more expensive technologies like the Silicon On Insulator, which presents several advantages for low-voltage applications [17]. In Figure 5, the charge pump presented in [16] is shown, as an example of the effort to improve the switched capacitor circuits: it is based on the well-known Favrat architecture [18] and it is basically

a cascade of simple two-phase voltage doubler. The charge transfer devices are composed of both pmos and nmos transistors: the latter ones are in triple-well to avoid breakdown. Another feature of the charge pump presented in [18] is that the voltage drop across each transistors is never higher than Vdd. This allows for using, instead of high-voltage transistors, the standard ones, which are highly preferable because of the reduced voltage threshold and parasitic capacitances.

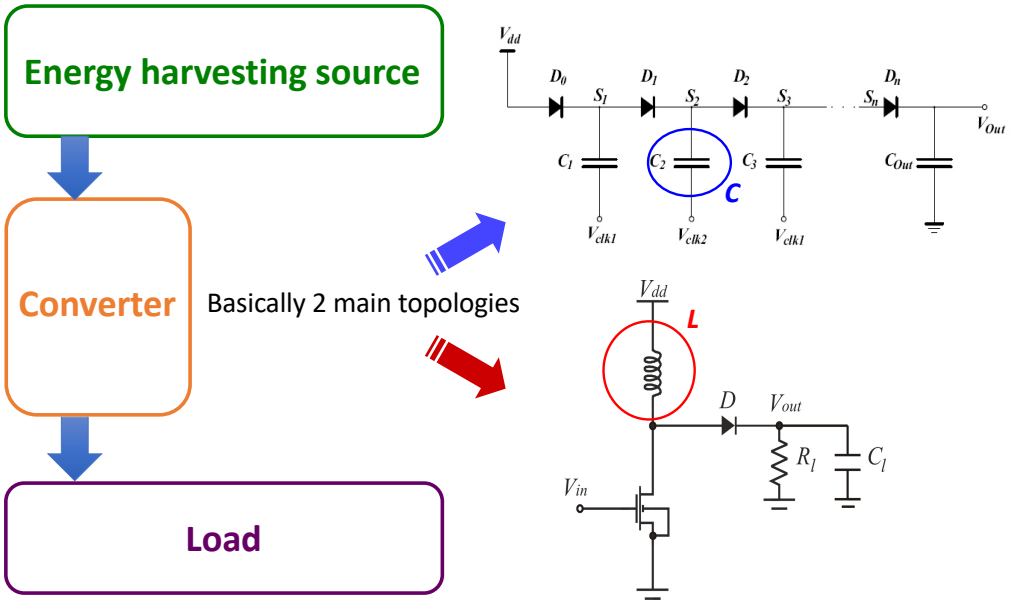

Figure 4. The main classical converter topologies.

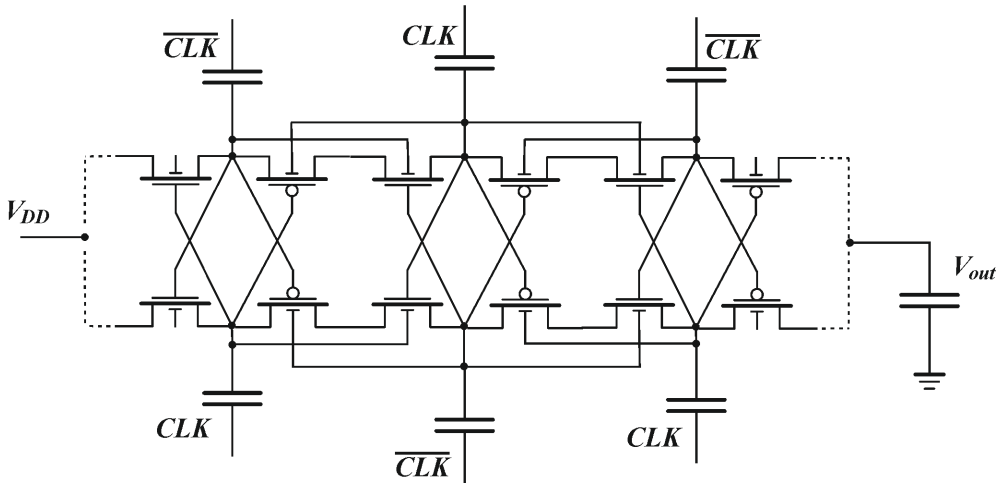

Figure 5. The switched capacitor converter presented in [16].

It is worth adding that the charge pump circuit is a particular type of switched capacitor converter (SCC) that can boost the input voltage. SCCs indeed can perform a wide range of conversion: they can indeed operate in step-up or boost, step-down or buck, and buck-boost way. The charge pumps are a particular type of SCC boost circuit. Several topologies of SCC can be found in the literature: the Ladder, the Cockcroft–Walton voltage multiplier, the Fibonacci, and the Series–Parallel converter. Their respective schematics are shown in Figure 6.

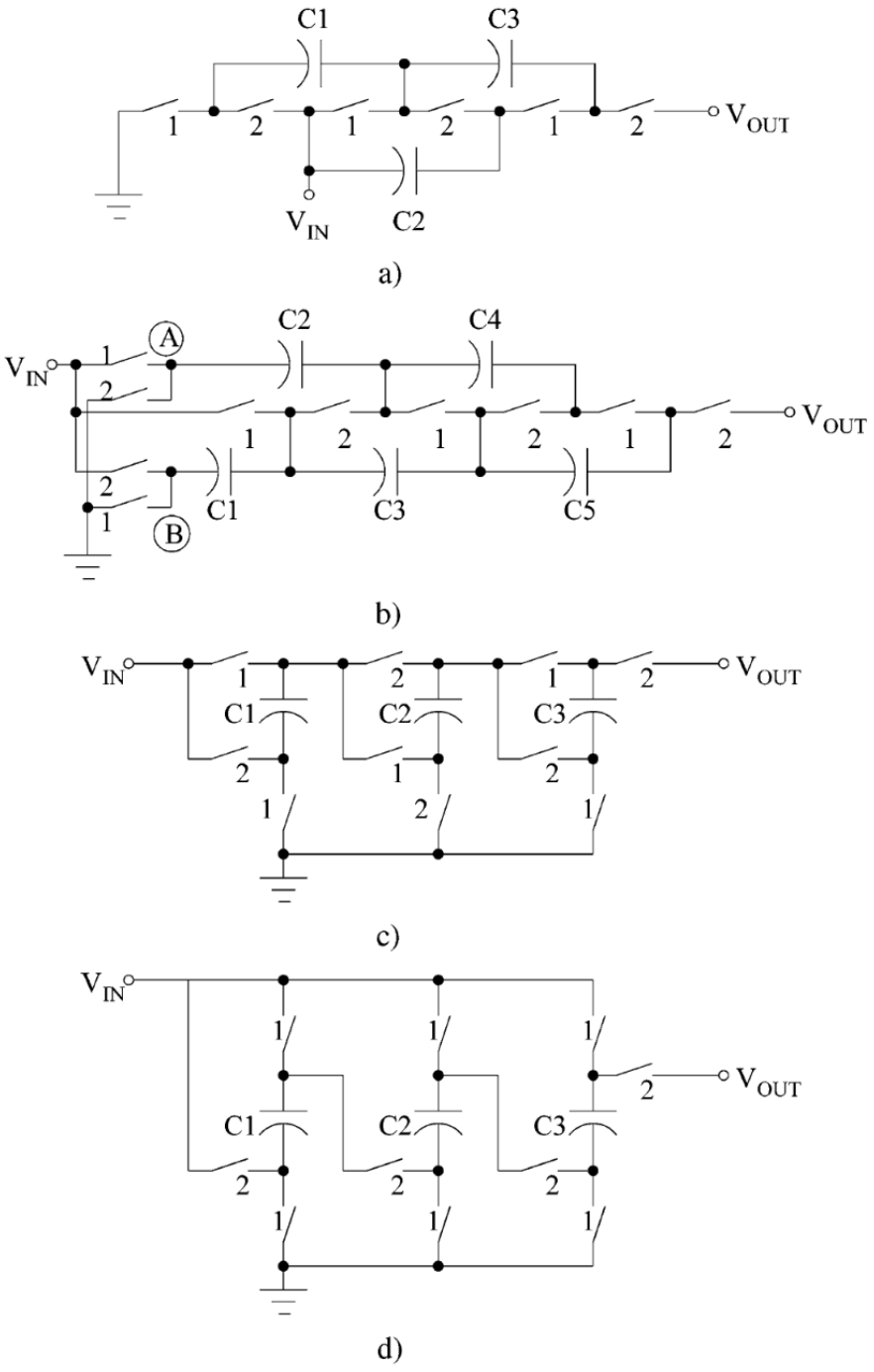

Figure 6. Different topologies of switched capacitor converters: (**a**) the Ladder, (**b**) the Cockcroft–Walton voltage multiplier, (**c**) the Fibonacci, and (**d**) the Series–Parallel converter.

A comprehensive analysis and comparison between these topologies can be found in the literature [19,20]. Topologies using SCCs have been adopted in low-power electronic applications, especially in systems with limited physical dimensions and involving high energy density. Their characteristics allow monolithic integration, minimized levels of electromagnetic interference (EMI), as well as reduced weight and volume. Unfortunately, despite the aforementioned advantages, the circuits based on only capacitors as energy buffer components cannot boost extremely low input voltages. Indeed, the output voltage can be maximized by increasing the number of steps of the charge pump, but this will degrade the power conversion efficiency and increase the circuit size. Regarding the expo-

nential converters (where the ratio of conversion is exponentially related to the number of capacitors), such as the Fibonacci, they exhibit poor performance. Furthermore, as the switches and capacitors used in their implementations support different voltage drops and most of the switches are not ground-referenced, it is difficult or near-impossible to achieve practical implementation. Moreover, these circuits may present low efficiency. This aspect is particularly influenced by the intrinsic characteristics of the switches and capacitors used in the circuit, and the number of components must also be carefully considered. The regulation of the load voltage is another challenge because, in certain operation conditions, the duty cycle does not have a linear relationship with the output voltage, which implies an increase in the complexity of the control systems. Contrarily, DC/DC converters based on inductive components are widely used in power electronics and recently they were integrated in CMOS standard process as well. The fully integrated inductive converter suffer from the limitation of low power efficiency because of the poor quality of the integrated inductor. In this kind of design, indeed, a realistic lumped model of the integrated inductor [21] is required. The inductor model should to be simple and must be based on linear passive components whose parameters are not dependent on the frequency; it should be able to account for current leakage of the substrate over a wide range of frequencies. The model must also be easily implementable in circuit simulators such as, for example, SPICE. Note that a reliable integrated inductor is area-limited, and therefore it can be only of tens of nH, at maximum. Therefore, the fully integrated inductive converters must be driven by fast clock signals, lossless devices, and large currents to achieve a large output voltage [22]. In [23], two step-up converters are cascade connected to reach a nominal value of 1.2 V starting from less than 200 mV, but it is worth noting that the inductors are external components of a few µH.

Another ultra-low-voltage step-up converter is proposed in [24]. Its design is aimed to operate with a minimum input voltage as low as 250 mV (this is the voltage range of most new sources of micro energy). A PCB prototype is realized and measured, showing a regulated maximum output voltage of 3.3 V. The architecture of the converter is made up of four major components: a differential oscillator, an intermediate DC-DC boost stage (IBS), a final boost stage, and a feedback control stage. The overall concept schematic is shown in Figure 7.

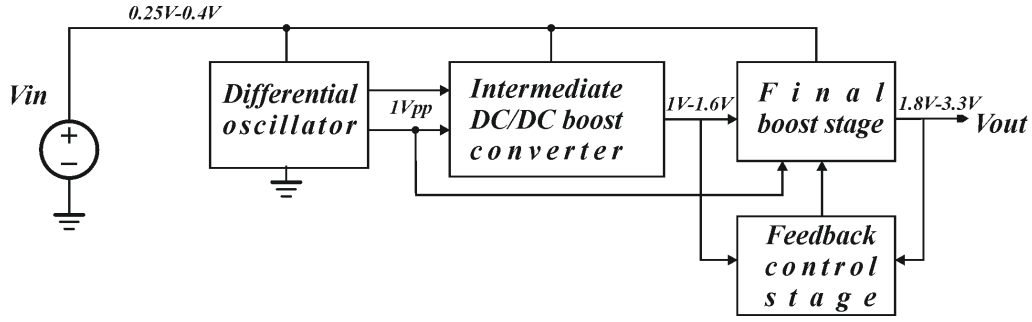

Figure 7. The inductive converter presented in [24].

Other topologies can be found in the literature [25–27]: they can efficiently boost very low input voltages, thanks to the use of a few external components (inductors, mechanical switches, or pre-charged capacitors).

The performance of DC/DC converters utilized in low-voltage systems can be improved by focusing on new designs that are based on both capacitive and inductive effects. Several architectures can be found in recent literature. For example, in [28], a hybrid converter is presented based on two main blocks: the first one is an inductive step-up which can boost a very low input voltage, driving the capacitors of the second stage which is a charge pump. The first stage is partially integrated: the inductors are indeed external

components; the second stage is instead fully integrated. For the sake of clarity, a concept schematic of this architecture is shown in Figure 8.

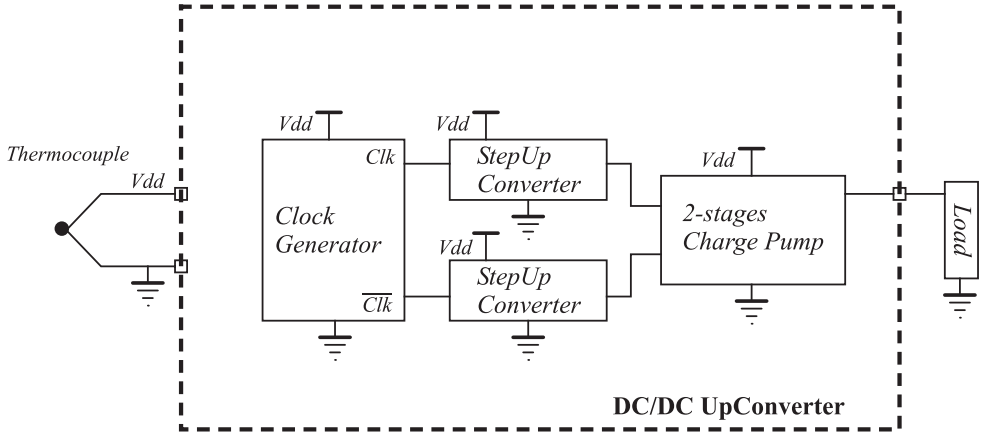

Figure 8. The hybrid converter presented in [28].

Many other hybrid topologies can be found in the literature: for example, a study presents a Dickson charge pump fully integrated DC/DC converter for use in low-voltage applications. The performance of this converter is improved in both power efficiency, rise time, voltage output ripple, and maximum output voltage thanks to the reliance of the systems to small integrated inductors [29]. Another study in [30] presents an autonomous self-starting ultra-low-voltage DC-DC converter that begins operations at 9 mV, and its circuit is based on JFETs used in a zero-voltage switching push–pull Royer oscillator (a relaxation oscillator based on a center-tapped transformer), to operate at low voltages. This topology of oscillator is simple, has a low number of components, an easy transformer isolation, and at the same time it ensures reduced weight and size of the transformer. The output of the classic Royer circuit is a square wave, that can be made harmonic by adding a resonant capacitor. Thanks to the symmetrical use of the transformer and the soft switching of the transistors, it can reach high voltage gain, high frequency, and high efficiency. In [31], a partially integrated DC/DC converter for ultra-low-voltage energy harvesting is presented, based on a hybrid capacitive and inductive system. It is composed of a transformer, a JFET switch, and an integrated CMOS charge pump. This architecture theoretically allows for converting extremely low-voltage inputs, which are the case, for example, of thermal energy harvesting: it can start at 6 mV without additional voltage supply nor pre-charged capacitors and at 30 mV of voltage supply it can provide 2.5 V output, delivering 250 µA to the load. It is worth adding that the transformer and the JFET switch are external components.

This converter is shown in Figure 9 for the sake of clarity. The charge pump acts as a rectifier, and it is improved by using the schematic on the right side of the figure. The study in [32] presents an autonomous system enabling thermal energy harvesting and power storage in the microwatt range. The architecture of the microsystem is made up of two sources of power: RF and thermoelectric; it also has a microbattery used as a storage unit and an IC for the transformation and management of the harvested energy and for interfacing with the microbattery. The thermogenerator in association with the DC/DC converter is used to charge the microbattery; it can also be charged using the external RF power that was converted by the RF converter. The output power of the thermal microgenerator is 411 W/cm^2 per °C, with a series resistance of a 90 Ω; it also generates 1V over a temperature gap of 60 °C. As shown in Figure 10, the micropower up-converter is used for the conversion of the power generated by the thermogenerator into a well-regulated power supply. The converter is based on a boost inductive converter, supplied by the 1 V thermogenerator and driven by an innovative pulse density modulator bootstrapped by means of a low-voltage, high-performance charge pump. It is partially integrated in a

0.35 µm CMOS technology and it can provide an output voltage of 1.75–4.3 V starting from a minimum 1V input voltage. The regulated voltage is 2.5 V and the maximum efficiency of the boost converter only is about 55%.

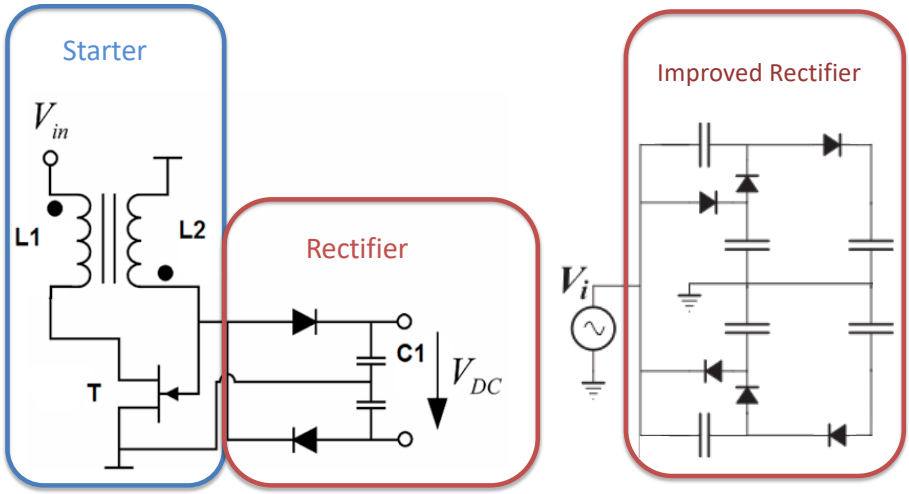

Figure 9. The hybrid converter presented in [31].

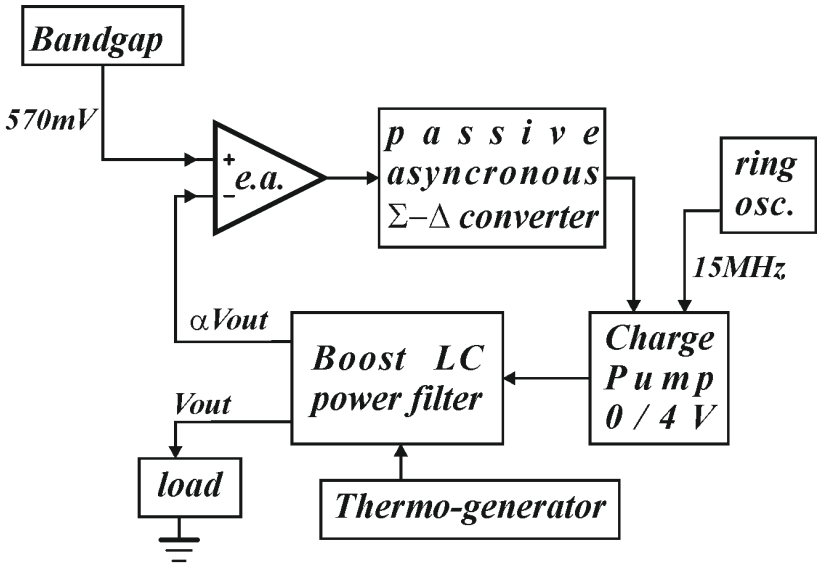

Figure 10. The hybrid converter presented in [32].

Another hybrid converter with lower startup voltage is presented in [33] and shown in Figure 11. To minimize the startup voltage, a capacitor pass-on scheme for the startup mechanism is proposed. The C_{OUT} is charged during start-up by the on-chip 20-stage Dickson charge pump that is driven by an on-chip CMOS oscillator. The latter is powered by a supply voltage of 95 mV, and it generates a 330 kHz clock signal. The output current during the startup is limited while the output capacitor is available for charging to a high voltage. When C_{OUT} is charged to the preset voltage, it is passed on with its charge inside to be the boost converter and supplies the control circuit. To turn on the power transistors MN and MP by using the control circuit, C_{OUT} should be charged to higher than their threshold voltage. The VT of the power transistors in this design is approximately 400 mV. Therefore, the preset voltage is designed to 460 mV to make sure the clock amplitude is enough to turn on the power transistors. By using the proposed scheme, the startup voltage can be reduced to 95 mV. The test chip of this hybrid converter has been fabricated

using 65 nm standard CMOS technology. An off-chip inductor of 6.8 µH and an off-chip capacitor of 10 nF are required by the circuit. The startup circuit is completely on-chip and the startup mechanism requires no extra devices. Measurement results show that the converter can deliver an output voltage of 0.9 V and an output current of ~1 mA. No data about the power efficiency are provided in manuscript [33].

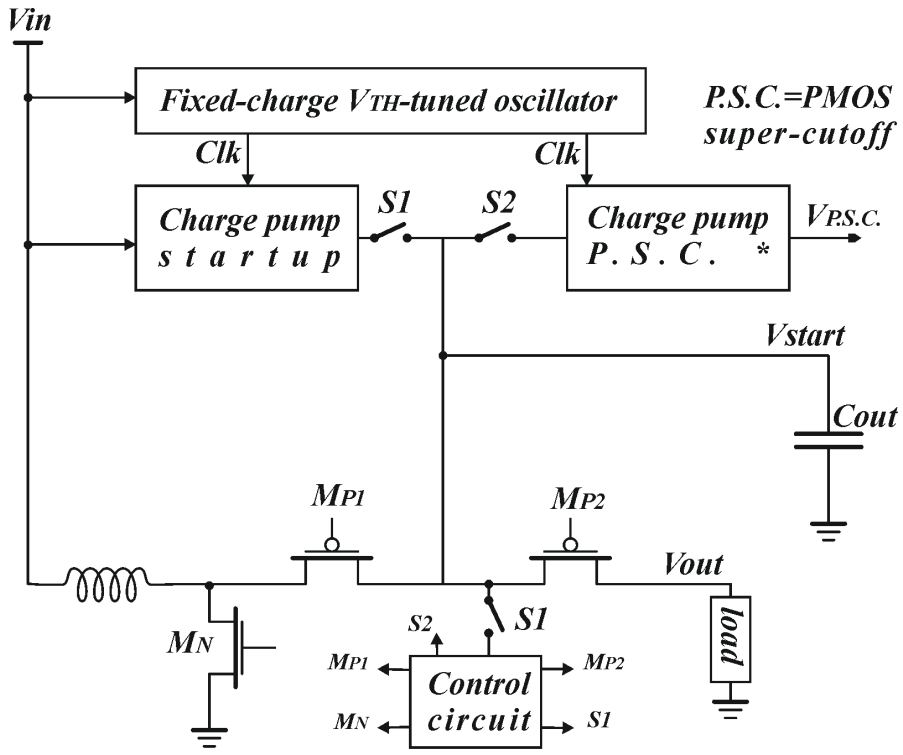

Figure 11. The hybrid converter presented in [33].

Although several other hybrid architectures can be found in the recent literature with specific conversion requirements (conversion ratio, efficiency, output current, output voltage, and so on), a special discussion must be devoted to the switched tank converters (STC) [34]. STCs aim to overcome the limits of the switched capacitor converters (SCCs). Among the critical limitations of SCCs, the charge redistribution is a well-known and investigated loss mechanism: the closing of a low-impedance switch between two capacitors causes a mismatch in the voltage between the capacitors, leading to charge redistribution and current inrush. Academics and researchers have proposed different derivative architectures to solve the problem of charge redistribution loss in the conventional SCCs. Most of these architectures are based on the introduction of some inductive elements into the SCCs to ensure that the charging and discharging process of the SCC flying capacitors are lossless. STCs are developed as a new and high-performing type of converters, based on capacitive and inductive elements, that can ensure easy control, scalability, and robustness against component nonidealities; they also ensure soft switching, complete soft charging, and minimal device voltage stresses in all operating conditions. STCs are composed of primary cells, or building blocks, having two major different structures, as shown in Figure 12. Practically, the energy in a STC is transferred between LC tanks or a dc filtering capacitor during switching instead of being switched and transferred between flying capacitors as in the conventional SCCs. This characteristic explains the topology name STCs.

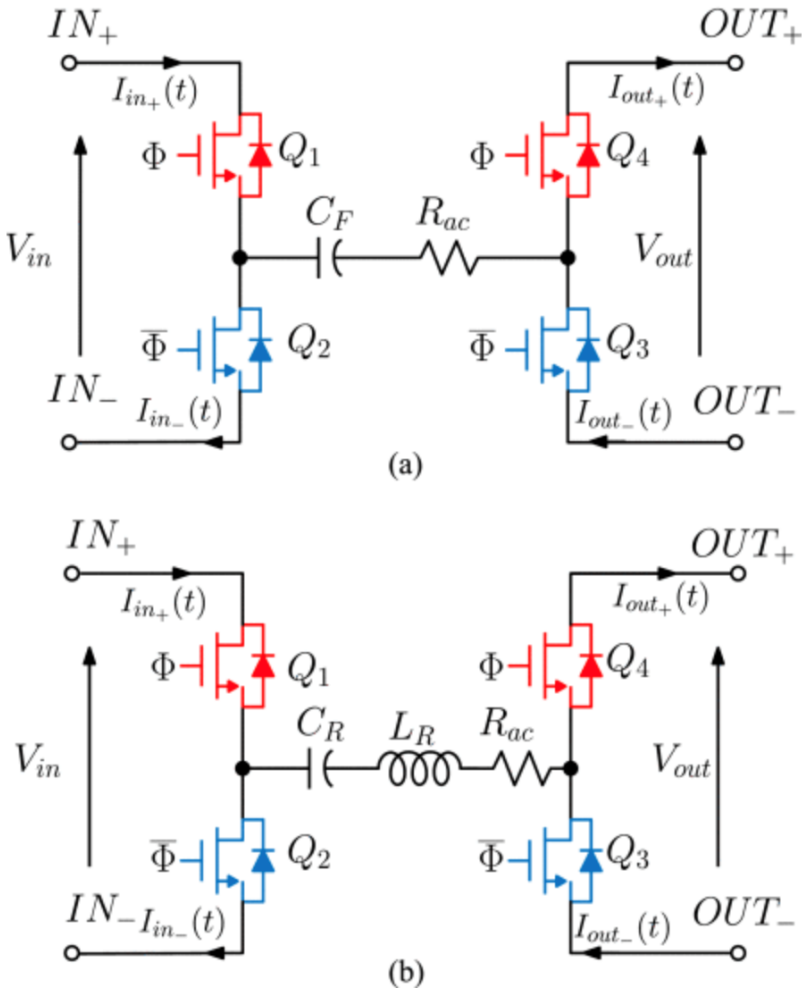

Figure 12. The buiding blocks of the STC presented in [34]: (**a**) structure with a clamping capacitor and (**b**) structure with a LC-resonant tank.

4. Converters' Topologies for Specific Harvesting Sources in IoT

The possible sources for energizing an IoT node can be, between the other ones, solar, thermal, vibration, or wind. Several projects of converters designed for these specific sources can be found in the literature. Indeed, the converters must present particular characteristics, like minimum starting input voltage level, input impedance, voltage ratio, and so on, depending on the specific energy harvesting source.

4.1. Converters for Energy from Thermoelectric Generator

As a first example, the energy scavenged from a thermoelectric generator (TEG) can be considered. In IoT applications, the TEG source is conceived to count on body-to-surrounding temperature difference (ΔT), and therefore a small ΔT is expected. A converter suitable for boosting TEG output voltage should be able to self-start and continue its energy harvesting at low TEG output voltage [35]. The study in [35] proposes the addition of a self-start assist circuit to the traditional self-start structure. The power converter is also equipped with maximum power point tracking (MPPT) feature for maximum power extraction from the TEG, and for providing a regulated output voltage. Figure 13 shows the schematic of the power converter that is made up of a self-start blocK, a main converter, an output stage, and two voltage detectors for VDDSS and VDDO, respectively. To achieve low start-up voltage without any additional components, a self-start circuit is used in the proposed system. The outputs of the self-start block, as shown in Figure 14, are a high-voltage HV_{SS} and a high-voltage swing clock CLK_{SS}. Both CLK_{SS} and HV_{SS} are used for the triggering of the main converter. The main converter continues power

extraction from TEG after self-starting and keeps charging the capacitor C_O to increase the VDDO output. The main converter output stage is regulated by the output stage to a stable output at different loads, and also for clamping the VDDO for self-protection.

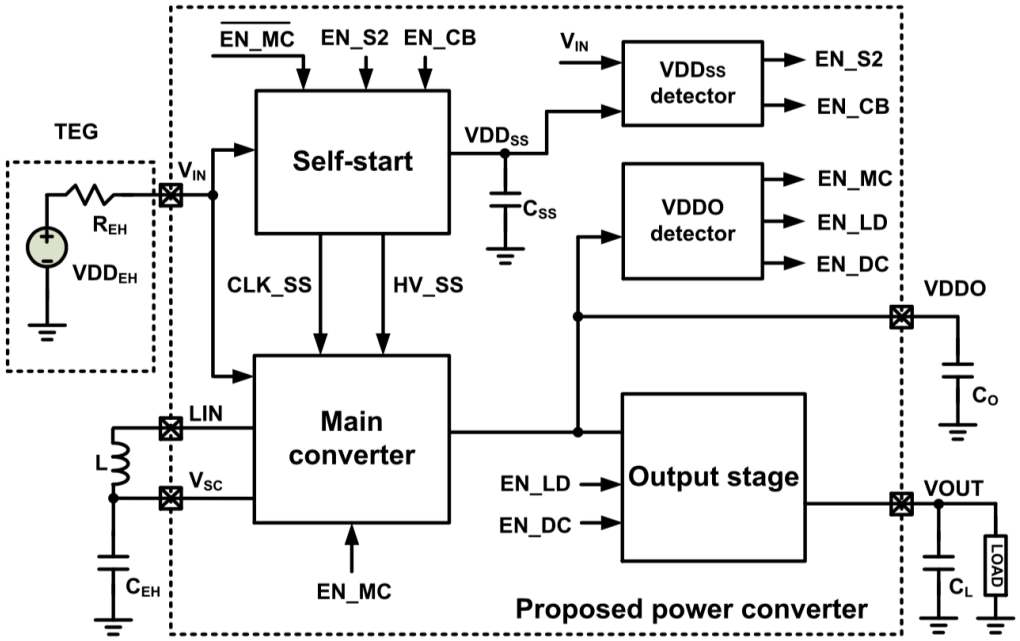

Figure 13. The hybrid converter presented in [35].

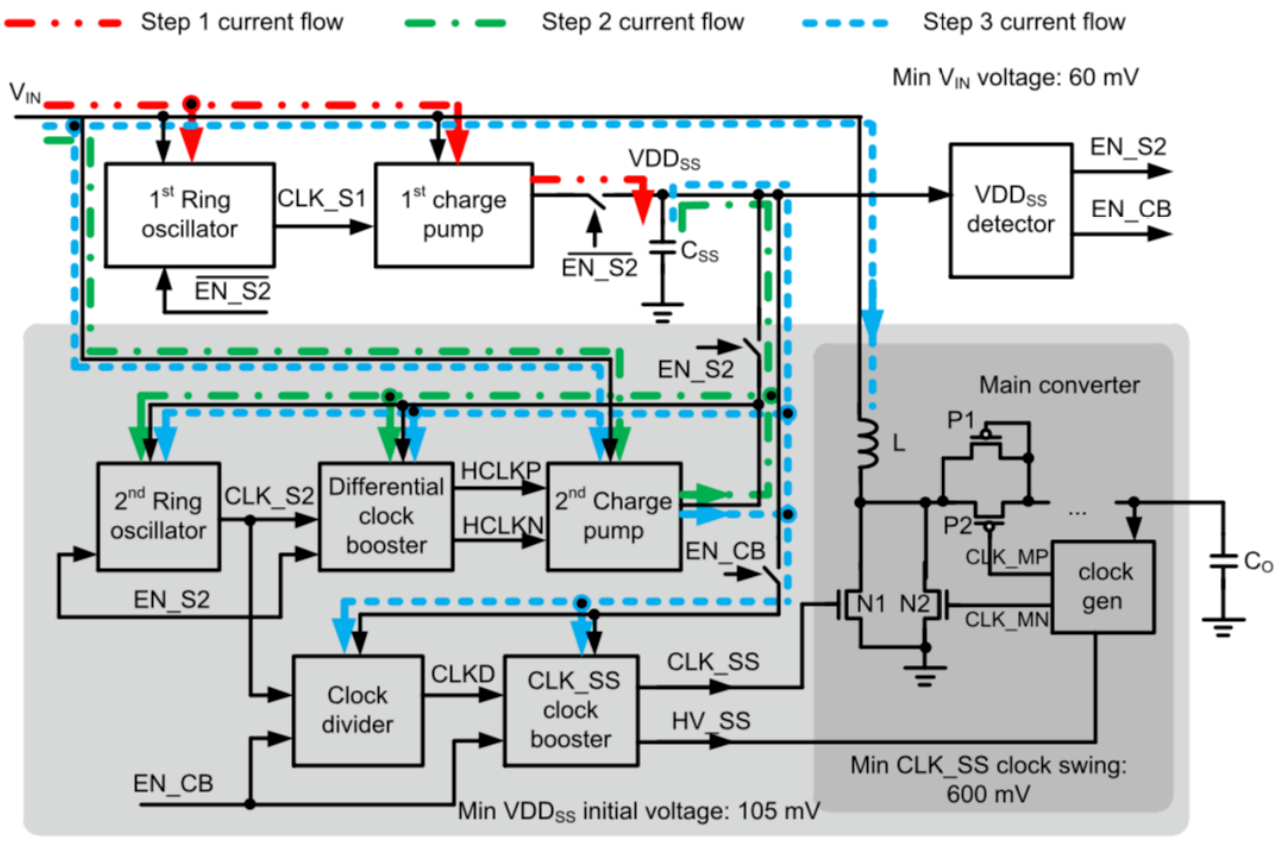

Figure 14. The self start-up block of the converter presented in [35].

Another work can be found in the literature [36,37] for converting the energy provided by a flexible thermoelectric generator (TEG). The system proposed in [36,37] is based on two integrated charge-pumps, fabricated in CMOS 130 nm technology. Figure 15 shows a schematic of the entire circuit system, with its two charge pumps: a low-power charge pump LP-CP operating in open loop, and another standard charge pump CP. Once V_{DD} goes beyond V_{DDmin}, an oscillator starts working to drive LP-CP for generating V_{1V} of about 1 V, which is regulated by a clamp circuit CLAMP. A bandgap reference BGR and some detectors are supplied by V_{1V}. The output voltage V_{ref} of the BGR is compared to the TEG output V_{DD}: if V_{DD} is enough, a first enabling signal is generated. The other enabling signals are addressed to the standard charge-pump CP, which generates V_{PP}, and to the ICs, which can work only when V_{PP} is sufficiently high.

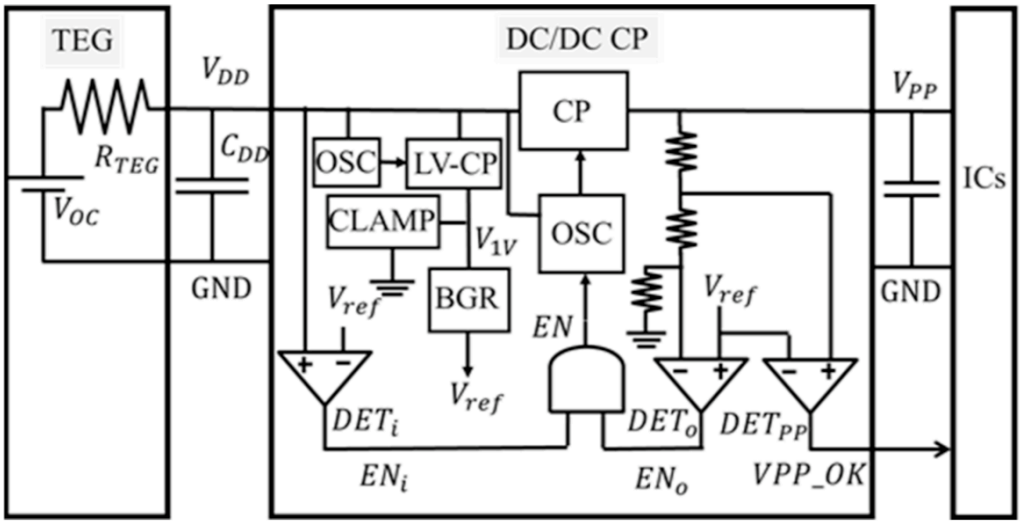

Figure 15. The double charge pump system presented in [36,37].

4.2. Converters for Energy from Solar Generator

The photovoltaic (PV) cell is mainly used recently due to its better efficiency and availability. PV cells have output voltage in the region from 0.45 to 0.7 V based on the environmental factors. Solar cells can serve as the input source, but, because they provide low voltage, they require boosting by a DC-DC converter. The study in [38] presents the design of an energy harvesting system (EHS) for boosting and regulating solar input voltage. It is simulated using the technology library of a CMOS 90 nm process. The components of the EHS include a non-overlapping clock generator with level shifter, a digital supply control oscillator, a DC-DC converter, an auxiliary charge pump, a current sensor, and a finite state machine (FSM) controller with maximum power point tracker (MPPT) module. For the sake of clarity, a schematic is shown in Figure 16.

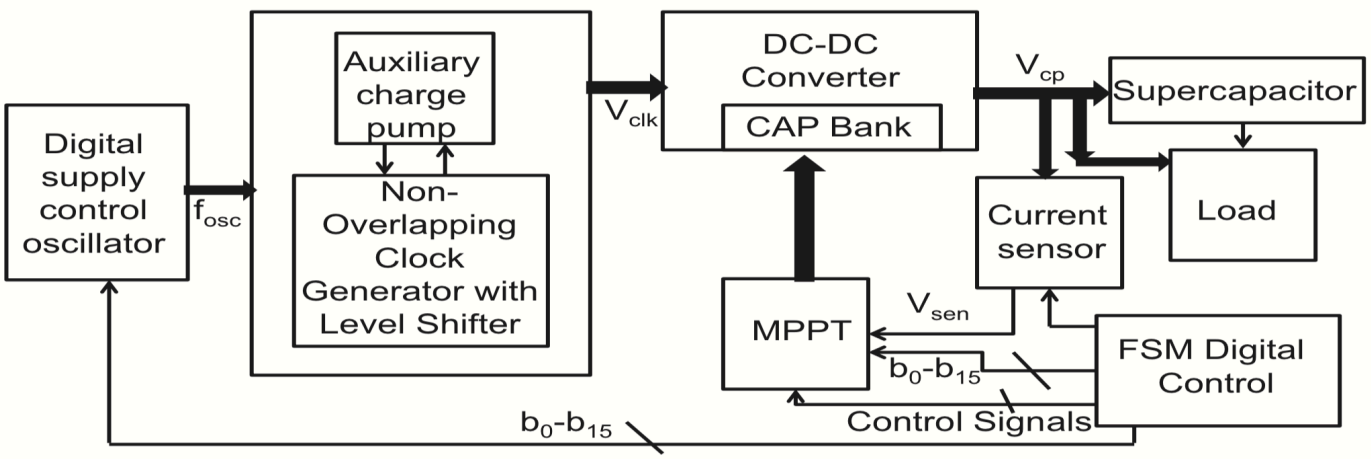

Figure 16. The concept schematic of the EHS presented in [38].

The charge pump boosts the voltage while the frequency tuning and capacitor value modulation ensure impedance matching between the converter and the solar cell. MPP is achieved using a hill-climbing technique; the EHS design is self-sustainable, with an output range of 3–3.55 V, and an input of 1–1.5 V. Another interesting work can be found in the recent literature dealing with the harvesting of indoor light [39]. Microwatts of power is generated by compact size PV cells under indoor lighting conditions, and this is not enough to power the mW RF power amplifier in IoT applications. On the other hand, in some applications (health and environment sensing, for example) the devices work in power-hungry active mode only for short periods (<1%) while staying in sleep mode for prolonged periods (>99%). Therefore, the microwatts of power, harvested from the indoor light, can be successfully used to energize the power-hungry RF amplifiers for a short period. In this case, an ad hoc converter must be designed. The work presented in [39] is focused on this kind of application: it employs a redistributable two-stage charge pump along with a storage capacitor. The role of the first stage is to track the MPP of the PV cell and to store the extracted energy in the storage capacitor, while the second stage regulates the voltage and boosts it to 1.5 V output. The size of the on-chip flying capacitors (CFLY) and the output voltage ripple are significantly reduced by partitioning the 2-stage CP into 16 sub-modules and by employing a multiphase interleaving technique. Fourteen submodules operate during the sleep mode to store the PV energy in the storage capacitor with MPPT, while the remaining submodules participate in state recycling to ensure a regulated output voltage of 1.5 V for the loading circuit. In active mode, all 16 submodules operate in the recycling state to convert VSTO to VOUT through the pulse-skip modulation technique (PSM). The concept schematic of the capacitive power converter, fabricated in 180 nm CMOS process, is shown in Figure 17.

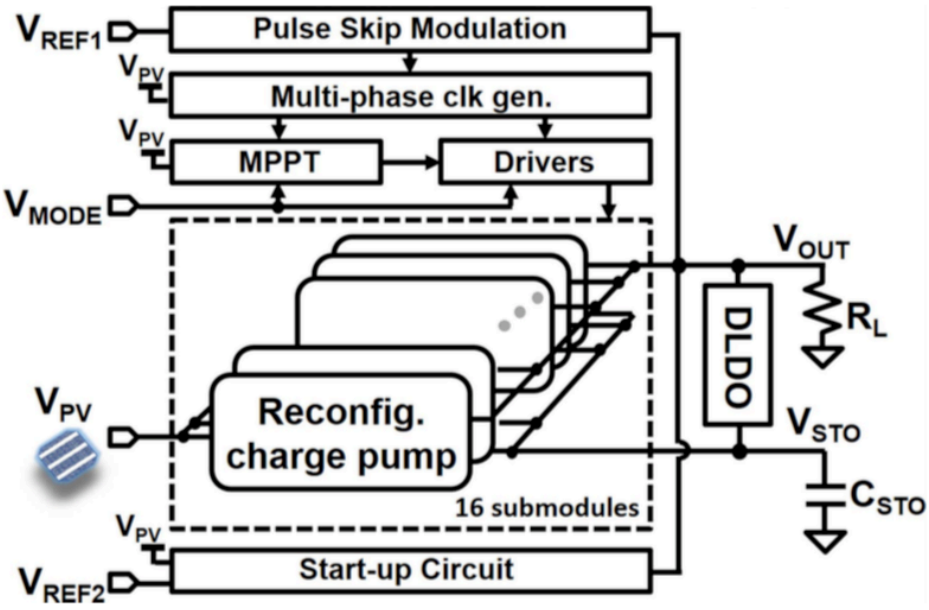

Figure 17. The concept schematic of the converter for indoor light presented in [39].

In [40], an optically-powered wireless tag, integrating a charge pump (CP) and a low-power RF transmitter for batteryless Internet-of-Things (IoT) applications, is presented. It is based on a CMOS charge pump with hysteresis regulation mechanism (HRM) which can power the transmitter circuit using indoor light energy.

An interesting comparison of the converter topologies (LDO, capacitive-based, and inductive converters) used for solar energy harvesting is discussed in [41]. Here, the comparison parameters are listed in Table 2, for the sake of completeness: the comparison highlights, between the others, terms like integrability and cost, which are very important in IoT applications.

Table 2. Comparison of DC/DC converter for solar energy harvesting.

Characteristics	LDO	Inductor-Based	Capacitor-Based
Type of converter	$V_{in} \geq V_{out}$	$V_{in} \geq$ or $\leq V_{out}$	$V_{in} \geq$ or $\leq V_{out}$
Efficiency	middle	very high	high
Load capacity	middle	high	middle
Ripple	very small	small	middle-large
EMI emission	very low	high	low
Integrability	very easy	difficult	easy
Complexity	low	middle-high	middle-high
Cost	low	middle	low-middle

4.3. Converters for Energy from RF Generator

Numerous RF signals abound in space due to the increasing use of wireless devices in various applications, such as TV or radio broadcasting, mobile phones, etc. Therefore, the available RF energy can be harvested and used to power IoT devices.

Wireless power transfer (WPT) can be achieved in two major ways as seen in Figure 18: near-field (non-radiative) technique and far-field (radiative) technique. Power transfer in the near-field technique is achieved using inductive coupling coils via magnetic fields. In this technique, the level of power transmission is in the range of μW to kW, and could be used for applications like smart watches, charging of mobile phones, medical implants,

and electric vehicles. However, the transmission distance of this technique is small, as the efficiency of power transfer diminishes with distance between the coils. Far-field WPT, on the other hand, is achieved through the EMW radiated by the antenna over a longer distance. Therefore, far-field WPT is the only technique that is suitable for IoT applications.

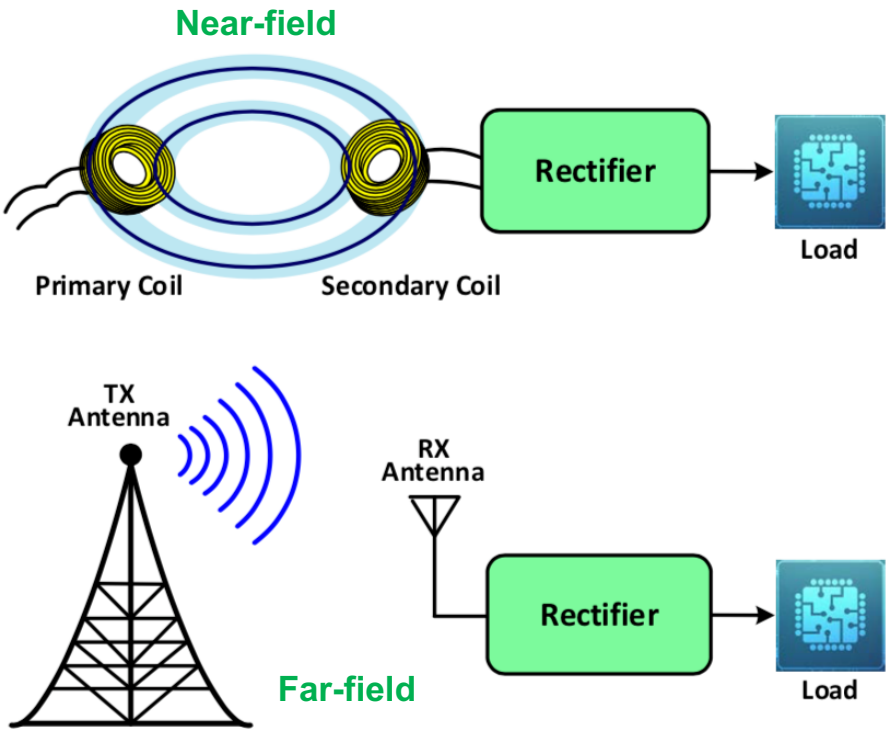

Figure 18. Wireless Power Transfer (WPT).

The component of a typical system for RF energy harvesting is made up of an antenna for the reception of ambient waves, an impedance matching network, power management units for the storage of the rectified energy, and an RF-to-DC converter. The ambient RF waves are converted by the antenna into electrical current. The mismatch between the impedance of the rectifier and the antenna, as well as the need for efficient power transfer to the rectifier, makes having a proper impedance matching network at the interface of both stages mandatory. The incoming RF power is then converted into dc power to supply the subsequent electronic circuitry. During the design of a RF energy harvesting systems, an important step is the selection of the suitable frequency band as this stage is reliant on the level of available power on the ambient for the potential application. The selected frequency band will have effect on the antenna size and on the impedance matching network. Therefore, the rectifier circuit must be optimized to the desired frequency band that the harvester system will operate upon. Thus, the rectifier circuit remains a major obstacle in determining the general performance of new RF harvester systems. Most rectifier circuits are based on Dickson charge pump model but there are reports of numerous on-chip rectifier circuits built in CMOS process [10,11,42,43]. For instance, the study in [43] presents a reconfigurable 2.45 GHz RF-DC converter that is fabricated in a 180 nm CMOS technology; the circuit system has been developed for efficient harvesting of electromagnetic energy. The components of the circuit include a low-power path rectifier, an adaptive path control (APC) circuit, and a high-power path rectifier. The components of the APC circuit include a comparator, an inverter, and two switches: it senses the output voltages of the high-power path and low-power path rectifiers for the generation of a control signal for auto-switching of the circuit between low and high power path operation based on the RF input power level. The circuit achieves more than 20% measured power conversion efficiency (PCE) from -6 dBm to 11 dBm input power range with maximum efficiencies of 41 and 45%,

respectively, at 1 and 6 dBm input powers, for 5 kΩ load resistance. The overall schematic is shown in Figure 19 for the sake of clarity.

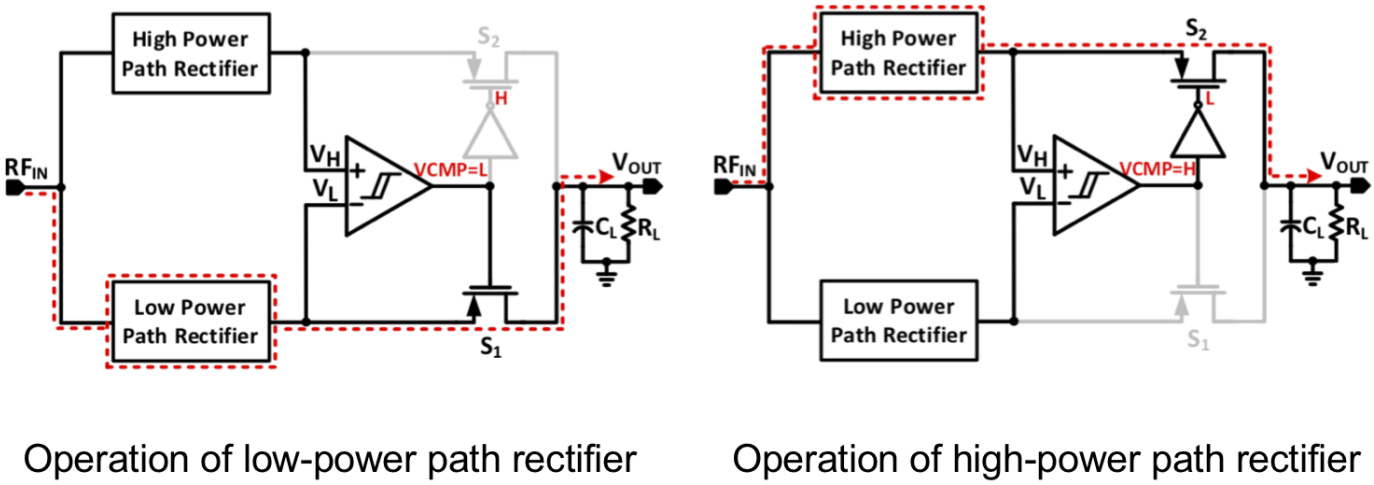

Figure 19. The RF-DC converter proposed in [43].

A power management circuit is presented in [44] for RF energy harvesters; the system is designed for possible integration in wireless sensor nodes. Efficient power transfer from a generic RF rectifier into a charge reservoir is achieved using a DC-DC boost converter, while a linear regulator is used to scale the voltage supply to the appropriate level for a sensing and conversion circuit. The power management system is implemented in a 65 nm CMOS technology, and it is found to achieve an overall efficiency of 20%, with the DC-DC converter having an input available power of 4.5 µW. The study in [45] discusses numerous designs and their trade-offs; it also analyzes the available RF energy harvesters. This work could guide future researchers on the trending areas in the field of RF energy harvesting.

4.4. Converters for Energy from Vibration and Wind Generators

Mechanical energy conversion from ambient vibrations into electrical energy is mostly efficient due to the ever-presence of vibrations and their higher power density. Vibrations with up to 1–50 Hz frequency range are mostly available in the environment, thereby making a low-frequency vibration energy harvester (VEH) attractive in the contest of wireless sensor nodes (WSNs). As shown in Figure 20, VEH is usually converted into an electrical energy using either electrostatic, electromagnetic (EM) transduction, or piezoelectric mechanisms. Many studies have been focused on the enhancement of the vibration energy harvesting process using these mentioned techniques [46].

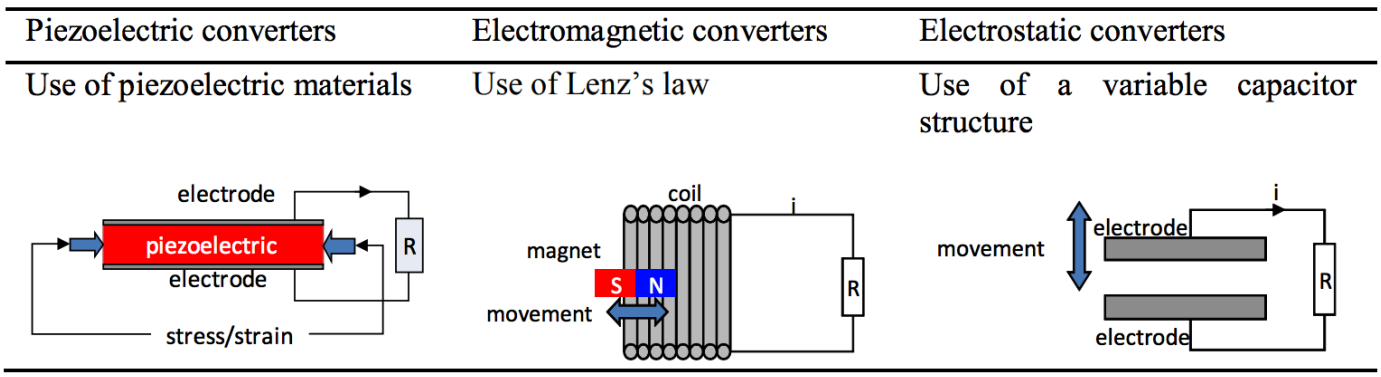

Figure 20. Different principles to convert mechanical energy into electricity [46].

VEH based on the piezoelectric effect is widely attractive due to the availability of well-performing piezoelectric materials and their potential higher power densities. EM VEHs have received much attention due to their high output voltage and large current [47]. Optimization of the harvesting mechanism also plays a significant role in improving the efficiency of the entire system. Due to the low voltage obtained from vibration, a power booster must be used, and numerous boost schemes have been suggested for VEH, but the major issue is the need for discrete capacitors, diodes, and inductors due to the low-frequency operation of VEH. Despite the attractiveness of these systems for IoT applications, their full integration for low-voltage output VEH is not an easy task. Therefore, in this paper, the work presented in [48] is mentioned: the power generated by VEH is rectified by a full-bridge rectifier (FBR), composed of a cross-coupled CMOS bridge circuit; the generated clock frequency (f_{CLK}) is increased by a ring oscillator (ROSC) and drives a charge pump (CP). Figure 21 shows the overall circuit fabricated in a 65 nm 1.0 V CMOS technology without requiring any external components.

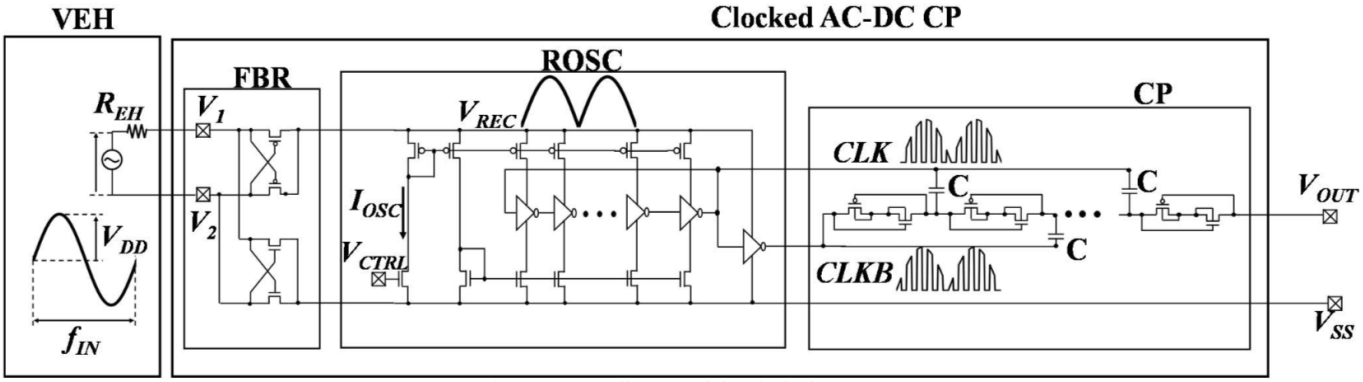

Figure 21. The fully integrated AC-DC converter presented in [48].

It is worth adding now that another kind of mechanical energy which can be converted into electricity is wind energy; it is also suitable and available, but not yet fully exploited at small scale, for powering low-power electronic systems such as Internet of Things (IoT) systems. The study in [49] interestingly introduces a three-phase mini wind energy harvester that incorporates a single stage AC/DC converter for improved efficiency and energy transfer.

5. DC/DC Converters for Multiple Energy Sources

In this section, an overview of the recent architectures and techniques focusing in energy harvesting from multiple heterogeneous sources is provided [50–55]. Energy harvesting from multiple sources is a more robust method for powering Internet of Things (IoT) nodes and similar wireless systems compared to harvesting from a single source. Renewable energy sources are, indeed, intermittent and fluctuating, but still inexhaustible and clean; if more than one energy source is combined, then intermittent supply from the renewable sources can be converted to continuous supply. Therefore, the multi-input (MI) DC–DC converter is a solution to overcome this problem. DC sources can be connected in series to implement an MI DC/DC converter; however, if one of the sources is discharged, it is difficult to obtain a regulated output voltage. DC sources can also be connected in parallel by means of a coupled transformer; the limitation of these topologies is that only one power source can transfer energy to the load at a time to prevent power coupling effects and the transformer must be suitably large to accommodate all windings. To overcome these difficulties, in [50], a simple MI non-isolated boost converter is proposed. It exploits a hybrid boost and switched-capacitor technique to provide a high-voltage gain and reduced switch stress. The topology and the behavior of the converter are similar to the traditional single input boost converter: this allows for an easy control strategy. A relevant feature of the circuit is that the output voltage is the same of twin/multiple boost converters

with the output circuits connected in series [51], but the switches are connected in parallel to the ground and no transformer is required. It significantly simplifies the gate voltage biasing and eventually digital control. In Figure 22, the dual-input schematic of the MI converter is shown, for the sake of clarity.

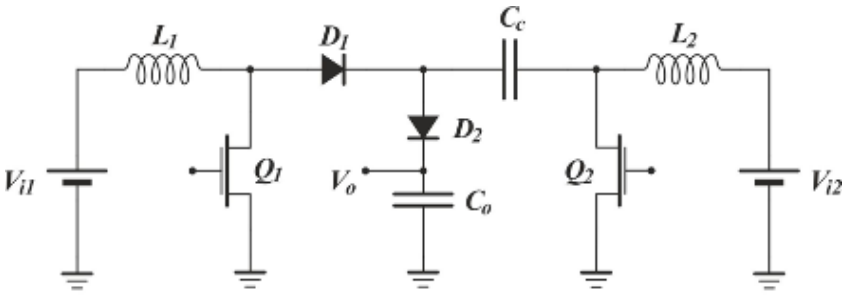

Figure 22. The MI DC-DC converter presented in [50], in the case of dual-input.

Another interesting work is discussed in [52]. It aims to design a two-stage MI energy harvesting DC adder combiner. The converter utilizes the DC outputs from PV, TEG, and rectified RF sources. Bypass transmission gates are added to each stage to simplify the management of the different availabilities of the three inputs. The core of the circuit is based on cross-coupled DC combiner stages which are based on a modified and improved version of the cross-coupled charge pump [16,18], with the adding of a first level gate control ensuring a proper off state at dead time periods, during the transitions of the clock from low to high or high to low. The paper provides the results of the design simulation and chip layout; SYNOPSYS Custom Designer simulation and layout tool implemented in TSMC 65 nm CMOS Process Technology are used. In Figure 23, the concept schematic of the MI DC adder combiner is shown.

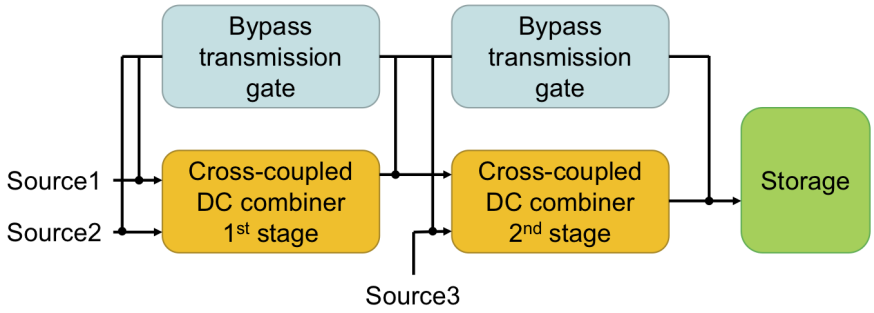

Figure 23. The concept adder combiner presented in [52].

A dual-input dual-output DC–DC converter (DIDC) topology is introduced in [54]; the proposed system can operate in single- and dual-input modes, as well as in dual-output mode using two energy sources. The system is developed using a single inductor, and fewer switches and other passive components, and it achieves low power losses and high level of reliability as an energy harvester. The DIDC converter operates in two phases. The operation in the first phase is with two inputs as the load is supplied by both photovoltaic (V_{PV}) and battery (V_b). In this mode, the battery is discharging. The second phase involves the converter operation with two outputs and V_{PV} supplies the load and charges the battery. The schematic of the DIDC converter is shown in Figure 24.

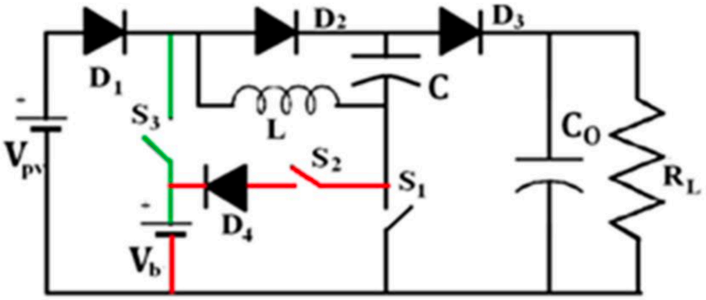

Figure 24. The DIDC topology presented in [54].

Last, the study in [55] describes the process of computer aided design (CAD) tool optimization for reconfigurable capacitive DC-DC converters with numerous inputs of different power levels. For each converter configuration, the theoretical maximum efficiency and the associated input power condition are estimated by this tool.

6. Conclusions

The emergence of IoT has driven the connection of numerous objects to the Internet, paving the way for the development of numerous smart and interconnected objects. However, numerous practical problems are yet to be addressed and a major one among them is the power supply. Therefore, several topologies of power converters and power management techniques have been considered and discussed in this paper, summarizing the main characteristics. The first topic to be discussed was the power consumption of the particular IoT node, and the second topic included the presentation of several general, classical, and recent DC/DC architectures. The designer has a wide range of possible converter topologies (SCCs, Inductive, Hybrid, or STCs). They can select the best one by considering the area, the efficiency, and so on. For example, SCCs are preferable for area and integrability, but switched inductors are better for the easy control of the output voltage. Finally, a section has been dedicated to the converters devised for special cases of energy harvesting. Indeed, the energy extracted from the environment is a kind of raw energy, which must be converted and stored to be useful in an electrical system, and therefore the choice of the converter will be oriented toward topologies operating with the smallest input voltage level, or toward modular and multiple input sources converters, which are preferable to better exploit energy from the environment.

Author Contributions: The authors contributed equally to this work. Conceptualization, methodology and investigation were done by A.R., M.S. and L.C.; original draft preparation was done by A.R.; review and editing was done by M.S. All authors have read and agreed to the published version of the manuscript.

Funding: This research received no external funding.

Institutional Review Board Statement: Not applicable.

Informed Consent Statement: Not applicable.

Conflicts of Interest: The authors declare no conflict of interest.

References

1. Lhermet, H.; Condemine, C.; Plissonnier, M.; Salot, R.; Audebert, P.; Rosset, M. Efficient Power Management Circuit: Thermal Energy Harvesting to Above-IC Microbattery Energy Storage. In Proceedings of the 2007 IEEE International Solid-State Circuits Conference, Digest of Technical Papers, San Francisco, CA, USA, 11–15 February 2007; pp. 62–587.
2. Cuadras, A.; Gasulla, M.; Ferrrari, V. Thermal energy harvesting through pyroelectricity. *Sens. Actuators A Phys.* **2010**, *158*, 132–139. [CrossRef]
3. Chai, R.; Zhang, Y. A Practical Supercapacitor Model for Power Management in Wireless Sensor Nodes. *IEEE Trans. Power Electron.* **2015**, *30*, 6720–6730. [CrossRef]

4. Kutbee, A.T.; Ghoneim, M.T.; Ahmad, S.M.; Hussain, M.M. Free-Form Flexible Lithium-Ion Microbattery. *IEEE Trans. Nanotechnol.* **2016**, *15*, 402–408. [CrossRef]
5. Chang, K. Bluetooth: A viable solution for IoT? [Industry Perspectives]. *IEEE Wireless Commun.* **2014**, *21*, 6–7. [CrossRef]
6. Martinez, B.; Montón, M.; Vilajosana, I.; Prades, J.D. The Power of Models: Modeling Power Consumption for IoT Devices. *IEEE Sens. J.* **2015**, *15*, 5777–5789. [CrossRef]
7. Hossein Motlagh, N.; Mohammadrezaei, M.; Hunt, J.; Zakeri, B. Internet of Things (IoT) and the Energy Sector. *Energies* **2020**, *13*, 494. [CrossRef]
8. Guegan, L.; Orgerie, A. Estimating the End-to-End Energy Consumption of Low-Bandwidth IoT Applications for WiFi Devices. In Proceedings of the 2019 IEEE International Conference on Cloud Computing Technology and Science (CloudCom), Sydney, NSW, Australia, 11–13 December 2019; pp. 287–294.
9. Dickson, J.F. On-chip high-voltage generation in MNOS integrated circuits using an improved voltage multiplier technique. *IEEE J. Solid-State Circuits* **1976**, *11*, 374–378. [CrossRef]
10. Richelli, A.; Colalongo, L.; Mensi, L.; Cacciatori, A.; Kovacs-Vajna, Z.M. Charge Pump Architectures Based on Dynamic Gate Control of the Pass-Transistors. *IEEE Trans. Very Large Scale Integr. Syst.* **2009**, *17*, 964–967. [CrossRef]
11. Ballo, A.; Grasso, A.D.; Palumbo, G. A Review of Charge Pump Topologies for the Power Management of IoT Nodes. *Electronics* **2019**, *8*, 480. [CrossRef]
12. Ballo, A.; Grasso, A.D.; Palumbo, G. A Subthreshold Cross-Coupled Hybrid Charge Pump for 50-mV Cold-Start. *IEEE Access* **2020**, *8*, 188959–188969. [CrossRef]
13. Rahman, L.F.; Marufuzzaman, M.; Alam, L.; Mokhtar, M.B. Design Topologies of a CMOS Charge Pump Circuit for Low Power Applications. *Electronics* **2021**, *10*, 676. [CrossRef]
14. Lin, H.; Chan, W.C.; Lee, W.K.; Chen, Z.; Chan, M.; Zhang, M. A High Conversion Ratio Component-Efficient Charge Pump for Display Drivers. *J. Display Technol.* **2016**, *12*, 1057–1063. [CrossRef]
15. Zhang, X.; Lee, H. Gain-Enhanced Monolithic Charge Pump With Simultaneous Dynamic Gate and Substrate Control. *IEEE Trans. Very Large Scale Integr. Syst.* **2013**, *21*, 593–596. [CrossRef]
16. Pelliconi, R.; Iezzi, D.; Baroni, A.; Pasotti, M.; Rolandi, P.L. Power efficient charge pump in deep submicron standard CMOS technology. *IEEE J. Solid-State Circuits* **2003**, *38*, 1068–1071. [CrossRef]
17. Biswas, A.; Sinangil, Y.; Chandrakasan, A.P. A 28 nm FDSOI Integrated Reconfigurable Switched-Capacitor Based Step-Up DC-DC Converter With 88% Peak Efficiency. *IEEE J. Solid-State Circuits* **2015**, *50*, 1540–1549. [CrossRef]
18. Favrat, P.; Deval, P.; Declercq, M.J. A high-efficiency CMOS voltage doubler. *IEEE J. Solid-State Circuits* **1998**, *33*, 410–416. [CrossRef]
19. Seeman, M.D.; Sanders, S.R. Analysis and Optimization of Switched-Capacitor DC–DC Converters. *IEEE Trans. Power Electron.* **2008**, *23*, 841–851. [CrossRef]
20. De Souza, A.F.; Tofoli, F.L.; Ribeiro, E.R. Switched Capacitor DC-DC Converters: A Survey on the Main Topologies, Design Characteristics, and Applications. *Energies* **2021**, *14*, 2231. [CrossRef]
21. Savio, A.; Carmina, M.; Richelli, A.; Colalongo, L.; Kovacs-Vajna, Z.M. A new lumped model for on-chip inductors including substrate currents. In Proceedings of the 12th IEEE International Conference on Fuzzy Systems, Cairo, Egypt, 11 December 2003; pp. 180–183.
22. Richelli, A.; Colalongo, L.; Quarantelli, M.; Carmina, M.; Kovacs-Vajna, Z.M. A fully integrated inductor-based 1.8-6-V step-up converter. *IEEE J. Solid-State Circuits* **2004**, *39*, 242–245. [CrossRef]
23. Richelli, A.; Comensoli, S.; Kovacs-Vajna, Z.M. A DC/DC Boosting Technique and Power Management for Ultralow-Voltage Energy Harvesting Applications. *IEEE Trans. Ind. Electron.* **2012**, *59*, 2701–2708. [CrossRef]
24. Bertacchini, A.; Scorcioni, S.; Cori, M.; Larcher, L.; Pavan, P. 250 mV Input Boost Converter for Low Power Applications. In Proceedings of the 2010 IEEE International Symposium on Industrial Electronics, Bari, Italy, 4–7 July 2010; pp. 533–538.
25. Damaschke, J.M. Design of a Low-Input-Voltage Converter for Thermoelectric Generator. *IEEE Trans. Ind. Appl.* **1997**, *33*, 1203–1207. [CrossRef]
26. Carlson, E.J.; Strunz, K.; Otis, B.P. A 20 mV Input Boost Converter With Efficient Digital Control for Thermoelectric Energy Harvesting. *IEEE J. Solid-State Circuits* **2010**, *45*, 741–750. [CrossRef]
27. Ramadass, Y.K.; Chandrakasan, A.P. A Battery-Less Thermoelectric Energy Harvesting Interface Circuit With 35 mV Startup Voltage. *IEEE J. Solid-State Circuits* **2010**, *46*, 333–341. [CrossRef]
28. Richelli, A.; Colalongo, L.; Tonoli, S.; Kovacs-Vajna, Z.M. A 0.2−1.2 V DC/DC Boost Converter for Power Harvesting Applications. *IEEE Trans. Power Electron.* **2009**, *24*, 1541–1546. [CrossRef]
29. Zucchelli, M.; Colalongo, L.; Richelli, A.; Kovacs-Vajna, Z.M. Dickson charge pump using integrated inductors in complementary metal–oxide semiconductor technology. *IET Power Electron.* **2016**, *9*, 553–558. [CrossRef]
30. Colalongo, L.; Leu, D.I.; Richelli, A.; Kovacs, Z. Ultra-Low Voltage Push-Pull Converter for Micro Energy Harvesting. *IEEE Trans. Circuits Syst. Express Briefs* **2020**, *67*, 3172–3176. [CrossRef]
31. Richelli, A.; Colalongo, L.; Kovacs-Vajna, Z. A 30 mV–2.5 V DC/DC converter for energy harvesting. *J. Low Power Electron.* **2015**, *11*, 190–195. [CrossRef]
32. Lhermet, H.; Condemine, C.; Plissonnier, M.; Salot, R.; Audebert, P.; Rosset, M. Efficient Power Management Circuit: Thermal Energy Harvesting to Above-IC Microbattery Energy Storage. *IEEE J. Solid-State Circuits* **2008**, *43*, 246–255. [CrossRef]

33. Po-Hung, C.; Ishida, K.; Ikeuchi, K.; Xin, Z.; Honda, K.; Okuma, Y.; Ryu, Y.; Takamiya, M.; Sakurai, T. Startup Techniques for 95 mV Step-Up Converter by Capacitor Pass-On Scheme and VTH -Tuned Oscillator With Fixed Charge Programming. *IEEE J. Solid-State Circuits* **2012**, *47*, 1252–1260.
34. Jiang, S.; Saggini, S.; Nan, C.; Li, X.; Chung, C.; Yazdani, M. Switched Tank Converters. *IEEE Trans. Power Electron.* **2019**, *34*, 5048–5062. [CrossRef]
35. Luo, Z.; Zeng, L.; Lau, B.; Lian, Y.; Heng, C. A Sub-10 mV Power Converter With Fully Integrated Self-Start, MPPT, and ZCS Control for Thermoelectric Energy Harvesting. *IEEE Trans. Circuits Syst. Regul. Pap.* **2018**, *65*, 1744–1757. [CrossRef]
36. Koketsu, K.; Tanzawa, T. A Design of Cold Start Charge Pump for Flexible Thermoelectric Generator with High Output Impedance. In Proceedings of the 2020 27th IEEE International Conference on Electronics, Circuits and Systems (ICECS), Glasgow, UK, 23–25 November 2020.
37. Koketsu, K.; Tanzawa, T. Design of a Charge Pump Circuit and System with Input Impedance Modulation for a Flexible-Type Thermoelectric Generator with High-Output Impedance. *Electronics* **2021**, *10*, 1212. [CrossRef]
38. Ram, S.K.; Das, B.B.; Swain, A.K.; Mahapatra, K.K. Ultra-Low Power Solar Energy Harvester for IoT Edge Node Devices. In Proceedings of the 2019 IEEE International Symposium on Smart Electronic Systems (iSES) (Formerly iNiS), Rourkela, India, 16–18 December 2019; pp. 205–208.
39. Cheng, H.-C.; Chen, P.-H.; Su, Y.-T.; Chen, P.-H. A Redistributable Capacitive Power Converter for Indoor Light-Powered Batteryless IoT Devices. *IEEE Solid-State Circuits Lett.* **2020**, *3*, 350–353. [CrossRef]
40. Cheng, H.-C.; Chen, Y.-T.; Chen, P.-H.; Liao, Y.-T. An Optically-Powered 432 MHz Wireless Tag for Batteryless Internet-of-Things Applications. *IEEE Trans. Circuits Syst. Regul. Pap.* **2019**, *66*, 3288–3295. [CrossRef]
41. Luo, P.; Peng, D.; Wang, Y.; Zheng, X. Review of Solar Energy Harvesting for IoT Applications. In Proceedings of the 2018 IEEE Asia Pacific Conference on Circuits and Systems (APCCAS), Chengdu, China, 26–30 October 2018; pp. 512–515.
42. Taghadosi, M.; Albasha, L.; Quadir, N.A.; Rahama, Y.A.; Qaddoumi, N. High Efficiency Energy Harvesters in 65 nm CMOS Process for Autonomous IoT Sensor Applications. *IEEE Access* **2018**, *6*, 2397–2409. [CrossRef]
43. Khan, D.; Basim, M.; Shehzad, K.; Ain, Q.U.; Verma, D.; Asif, M.; Oh, S.J.; Pu, Y.G.; Yoo, S.-S.; Hwang, K.C.; et al. A 2.45 GHz High Efficiency CMOS RF Energy Harvester with Adaptive Path Control. *Electronics* **2020**, *9*, 1107. [CrossRef]
44. Caselli, M.; Ronchi, M.; Boni, A. Power Management Circuits for Low-Power RF Energy Harvesters. *J. Low Power Electron. Appl.* **2020**, *10*, 29. [CrossRef]
45. Khan, D.; Basim, M.; Shehzad, K.; Ain, Q.U.; Verma, D.; Asif, M.; Oh, S.J.; Pu, Y.G.; Yoo, S.-S.; Hwang, K.C.; et al. A Survey on RF Energy Harvesting System with High Efficiency RF-DC Converters. *J. Semicond. Eng.* **2020**, *1*, 13–30.
46. Boisseau, S.; Despesse, G.; Seddik, B.A. Electrostatic Conversion for Vibration Energy Harvesting. In *Small-Scale Energy Harvesting*; Lallart, M., Eds.; IntechOpen: London, UK, 2012. [CrossRef]
47. Qiu, J.; Liu, X.; Chen, H.; Xu, X.; Wen, Y.; Li, P. A Low-Frequency Resonant Electromagnetic Vibration Energy Harvester Employing the Halbach Arrays for Intelligent Wireless Sensor Networks. *IEEE Trans. Magn.* **2015**, *51*, 1–4.
48. Kawauchi, H.; Tanzawa, T. A 2 V 3.8 μW Fully-Integrated Clocked AC-DC Charge Pump with 0.5 V 500 Ω Vibration Energy Harvester. In Proceedings of the 2019 IEEE Asia Pacific Conference on Circuits and Systems (APCCAS), Bangkok, Thailand, 11–14 November 2019; pp. 329–332.
49. Pozo, B.; Araujo, J.Á.; Zessin, H.; Mateu, L.; Garate, J.I.; Spies, P. Mini Wind Harvester and a Low Power Three-Phase AC/DC Converter to Power IoT Devices: Analysis, Simulation, Test and Design. *Appl. Sci.* **2020**, *10*, 6347. [CrossRef]
50. Colalongo, L.; Dotti, D.; Richelli, A.; Kovács-Vajna, Z.M. Non-isolated multiple-input boost converter for energy harvesting. *Electron. Lett.* **2017**, *53*, 1132–1134. [CrossRef]
51. Caricchi, F.; Crescimbini, F.; Napoli, A.D.; Honorati, O.; Santini, E. Testing of a new D.C.–D.C. converter topology for integrated windphotovoltaic generating systems. In Proceedings of the European Conference Power Electronics and Applications, Brighton, UK, 13–16 September 1993; pp. 83–88.
52. Diangco, M.M.C.; Gerasta, O.J.L. Multiple-Input Energy Harvesting DC Adder Combiner for Internet of Things (IoT) Wireless Sensor Nodes (WSN) Applications in 65 nm CMOS Technology. In Proceedings of the 2019 IEEE 11th International Conference on Humanoid, Nanotechnology, Information Technology, Communication and Control, Environment, and Management (HNICEM), Laoag City, Philippines, 29 November–1 December 2019; pp. 1–6.
53. Estrada-López, J.J.; Abuellil, A.; Zeng, Z.; Sánchez-Sinencio, E. Multiple Input Energy Harvesting Systems for Autonomous IoT End-Nodes. *J. Low Power Electron. Appl.* **2018**, *8*, 6. [CrossRef]
54. Lavanya, A.; Jegatheesan, R.; Vijayakumar, K. Design of Novel Dual Input DC–DC Converter for Energy Harvesting System in IoT Sensor Nodes. *Wireless Pers. Commun.* **2021**, *117*, 2793–2808. [CrossRef]
55. Elabany, A.; Nassar, A.; Mostafa, H. Design Optimization of Multi-Input Reconfigurable Capacitive DC-DC Converters: A CAD Tool Approach. In Proceedings of the 2021 IEEE International Symposium on Circuits and Systems (ISCAS), Daegu, Korea, 22–28 May 2021; pp. 1–5.